Journal of Water Process Engineering 86 (2026) 109975

Contents lists available at ScienceDirect

Journal of Water Process Engineering

journal homepage: www.elsevier.com/locate/jwpe

Uncovering nitrogen removal in algal-bacterial processes for domestic wastewater treatment

Thalita Lacerda dos Santos [a,b], Laura Vargas-Estrada [a], Saúl Blanco [c], Gustavo Henrique Ribeiro da Silva [b], Raúl Muñoz [a,*]

[a] Institute of Sustainable Processes, University of Valladolid, Dr. Mergelina s/n., 47011, Valladolid, Spain
[b] São Paulo State University, Av. Eng. Luiz Edmundo C. Coube 14-01, 17033-360, Bauru (SP), Brazil
[c] University of León, Avenida de la Facultad, 25, 24004, León, Spain

ARTICLE INFO

Editor: Meng Wang

Keywords:
Algal–bacterial interactions
Nitrogen assimilation
Single-stage PBR
Biomass productivity

ABSTRACT

The synergy between microalgae and bacteria in photobioreactors is complex, with the competition between assimilation and nitrification critically influencing nutrient removal efficiency. This study investigated the interplay between nutrient and carbon removal pathways in a single-stage microalgal-bacterial photobioreactor treating domestic wastewater by selectively inhibiting nitrification with allylthiourea (ATU). The inhibition successfully suppressed bacterial activity, reducing the NH_4^+ removal rate by 20% and increasing the contribution of microalgal assimilation to total nitrogen removal from 59% to 68%. Moreover, ATU addition induced a change in microbial population structure, as suggested by the decline in relative abundance of Proteobacteria and Bacteroidota phyla, which ultimately mediated a shift in the share of carbon fate mechanisms. The total organic carbon removal efficiency decreased from 94 ± 1% to 88 ± 1%, while the carbon assimilation efficiency into biomass was increased from 65% to 80%. Thus, mixotrophic microalgae like *Scenedesmus* sp. became the dominant genus, alongside the cyanobacterium *Nodosilinea*. Phosphate removal remained consistently high (97–98%) and unaffected by ATU addition, indicating its decoupling from nitrification. The results demonstrated that nitrogen removal was mainly dominated by microalgae assimilation complemented by bacterial pathway, consistent with nitrification-denitrification to achieve complete nitrogen removal.

1. Introduction

The treatment and disposal of domestic wastewater represent a significant global challenge, driven by the increasing volumes generated, its potential contribution to greenhouse gas emissions and eutrophication, and urgent need for water reuse [1–3]. Conventional nutrient removal in wastewater treatment plants (WWTPs) is often energy intensive and inefficient in terms of resource recovery, particularly for domestic wastewaters with low C:N ratios and phosphorus concentrations [1,4,5].

Nitrogen transformation in biological wastewater treatment systems involves multiple pathways, including ammonification, nitrification, denitrification, assimilatory and dissimilatory nitrate reduction to ammonium, anammox, and nitrite-nitrate interconversion [2,6]. Of these, the nitrification-denitrification pathway is the most widely adopted for engineered biological nitrogen removal [1–3,6]. However, this multi-step process is energy-intensive due to the aeration demand for nitrification and the external carbon source requirements for heterotrophic denitrification [2,3]. In addition, an incomplete hydroxylamine oxidation (NH_2OH), nitrite reduction or an incomplete heterotrophic denitrification, can biologically produce N_2O, a potent greenhouse gas with a global warming potential 298 times greater than CO_2, posing a significant sustainability challenge for conventional biological processes [7–9].

As a sustainable alternative to activated sludge processes, microalgal-bacterial consortia offer several advantages, as the photosynthetically produced oxygen from the assimilation of inorganic carbon by microalgae can sustain the activity of ammonia-oxidising bacteria (AOB) and nitrite-oxidising bacteria (NOB) for nitrification. Hence, a simultaneous nitrogen and phosphorus removal, with potential for resource recovery as algal-bacterial biomass, can be carried out while addressing critical challenges of water scarcity [2,10–16].

In these systems, a fundamental competitive dynamic occurs: microalgae and AOB primarily utilize ammonium (NH_4^+) as their

* Corresponding author.
E-mail address: raul.munoz.torre@uva.es (R. Muñoz).

https://doi.org/10.1016/j.jwpe.2026.109975
Received 31 December 2025; Received in revised form 14 February 2026; Accepted 25 March 2026
Available online 30 March 2026

nitrogen source and nitrogen/electron donor source, respectively [1,17]. On one hand, the excess of oxygen produced by microalgae is used by AOB to oxidise NH_4^+ to NO_2^-, which is further oxidised to NO_3^- by NOB. These processes maintain minimal NH_4^+ concentrations in the cultivation broth and prevent microalgae inhibition while maintaining NO_3^- for microalgae assimilation [13]. Even if microalgae can assimilate nitrate, this pathway is typically less efficient than NH_4^+ uptake [18]. Hence, competition for ammonia governs the overall nitrogen removal efficiency and process stability [1,17,19]. Despite microalgae and nitrifiers can symbiotically coexist, their relationship involves complex interactions and specific operational parameters. Typically, nitrification is carried out by Proteobacteria and Bacteroidetes, with *Nitrosomonas* and *Nitrospira* typically identified as the key AOB and NOB species. Nonetheless their sensitivity to high light intensities could limit their presence in microalgae cultures [2]. In addition, the high DO concentrations resulting from photosynthetic microalgae metabolism can hinder the heterotrophic nitrate denitrification, which is a strictly anaerobic process. The dynamics and dominance of these pathways, which intersect with carbon removal mechanisms, remain poorly characterized, particularly in single-stage photobioreactors.

A particularly relevant mechanism in single-stage photobioreactors, especially when devoted to the treatment of wastewaters with a low C:N ratio, is the simultaneous nitrification-denitrification (SND). This biological mechanism involves aerobic autotrophic nitrifiers and aerobic denitrifiers, which possess the capacity to perform denitrification under oxygen-saturated conditions. On the other hand, SND can be also conducted by aerobic autotrophic nitrifiers and anaerobic heterotrophic denitrifiers when oxygen diffusion limitations create anoxic microniches, allowing the coexistence of both microbial groups [2]. To elucidate the occurrence of these interactions, allylthiourea (ATU), a well-established inhibitor of the key AOB enzyme ammonia monooxygenase (AMO), can be added to the algal-bacterial cultivation broth as an experimental tool to selectively inhibit nitrification and elucidate the mechanisms involving competition for nitrogen between microalgae and bacteria. Indeed, ATU chelates copper at its active site in AMO at specific concentrations, transiently inhibiting AOB activity without significantly affecting microalgal activity [13,20] and allowing to elucidate the occurrence of denitrification.

Therefore, the main objective of this study was to elucidate the respective contributions of nitrogen assimilation by microalgae and bacteria, and nitrification-denitrification by bacteria, by selectively inhibiting nitrification, providing critical insights for optimizing algal-bacterial wastewater treatment.

2. Materials and methods

2.1. Synthetic wastewater composition

Synthetic domestic wastewater (SWW) was used in this study to minimize compositional fluctuations inherent to real wastewater. SWW was prepared by modifying BG 11 medium [21] and using tap water. The SWW composition (per L) comprised: 0.625 g glucose, 0.7 g $NaHCO_3$, 0.16 g peptone, 0.11 g meat extract, 0.15 g NH_4Cl, 0.04 g K_2HPO_4, 0.075 g $MgSO_4.7H_2O$, 0.036 g $CaCl_2.2H_2O$, 0.02 g Na_2CO_3 and 1 mL of micronutrients solution composed of (per L): 6.0 g citric acid, 6.0 g ferric ammonium citrate, 1.0 g EDTA.Na_2, 2.86 g H_3BO_3, 1.81 g $MnCl_2.4H_2O$, 0.39 g $Na_2MoO_4.2H_2O$, 0.08 g $CuSO_4.5H_2O$, 0.05 g Co $(NO_3)_2.6H_2O$, 0.22 g $ZnSO_4.7H_2O$. The SWW had a pH of 8.1 ± 0.2 and concentrations of total organic carbon (TOC) of 360.2 ± 21.1 mg L^{-1}, inorganic carbon (IC) of 109.7 ± 5.1 mg L^{-1}, total nitrogen (TN) of 70.5 ± 7.8 mg L^{-1} and total phosphorus (TP) of 15.0 ± 2.6 mg L^{-1}, and theoretical concentrations of potassium (K) of 17.96 mg L^{-1}, calcium (Ca) 9.81 mg L^{-1}, zinc (Zn) 0.05 mg L^{-1}, magnesium (Mg) 7.40 mg L^{-1}, sulphur (S) 9.79 mg L^{-1}, and iron (Fe) 0.75 mg L^{-1}. The SWW was supplemented with 0.05 g L^{-1} of allyl-thiourea ($C_4H_8N_2S$) to inhibit nitrification, resulting in an inlet TN concentration of 85.9 ± 5.6 mg L^{-1}.

2.2. Inoculum

The PBR was inoculated with a microalgal-bacterial consortium, prepared by combining fresh aerobic activated sludge (AS) with a pre-adapted microalgal culture at a volume ratio of 1.0 L algal concentrate to 2.2 L AS broth, followed by dilution with SWW to the 22 L working volume. The AS was obtained from the activated sludge secondary settler of Valladolid wastewater treatment plant (WWTP), with a total suspended solids (TSS) concentration of 4.2 g L^{-1}. Valladolid WWTP operates with a nitrification-denitrification configuration. The microalgal inoculum was obtained from an indoor pond treating real centrate from the same WWTP as described elsewhere [22]. This initial consortium was subsequently acclimated to the SWW and agitation conditions for 192 days to select a robust algal-bacterial community adapted to the target operational parameters [23]. The structure of the photosynthetic population in the adapted algal-bacterial consortium was composed of *Scenedesmus* sp. (77%) and *Pseudanabaena* sp. (23%).

2.3. Experimental configuration and operational conditions

The experimental system consisted of an indoor column photobioreactor (PBR) (0.15 m diameter, 1.31 m height) constructed in methacrylate. The PBR was operated for 38 days under controlled light and temperature conditions. The culture broth within the PBR was agitated using two strategically located pumps (Eden 159 at the bottom; CompactON 300 in the upper third). Continuous illumination was set to eliminate the variability introduced by light-dark cycles and was provided by two high-intensity LED panels (Philips S.A., Poland) delivering an average photosynthetic active radiation (PAR) of 316.6 ± 9.9 μmol m^{-2} s^{-1}. The PBR was coupled to a 1 L conical settler (Fig. 1), which supported a settled biomass recirculation at a flow rate of 0.75 L d^{-1}.

Biomass concentration in the PBR was maintained below 2 g TSS L^{-1} by continuous withdrawal from the bottom of the settler. The volume withdrawn was centrifuged (4000 rpm, 20 min), the biomass pellet was discarded, whilst the supernatant was recycled to the PBR to preserve the mass balance. This operational strategy resulted in a solid retention time (SRT) of 3 ± 1 days. These operational conditions favoured the dominance of bacteria with high specific growth rates, thereby promoting partial nitrification without significant nitrite accumulation [13].

The 38-day experiment was divided in two sequential operational stages: an initial 23 days stage when the system was only feed with SWW, followed by a 15 days stage when ATU was added to the SWW at a concentration 0.05 g L^{-1} to inhibit nitrification. A hydraulic retention time (HRT) of 1 day was maintained throughout both operational stages.

2.4. Sampling and analytical procedures

Process parameters including pH (SensION™ + PH3 pHmeter, HACH, Spain), temperature (multiparameter analyser C-3020, Consort, Belgium) and dissolved oxygen (DO, OXI 3310 oximeter, WTW, Germany) were daily monitored at 11:00 a.m. PAR was measured weekly using a LI-250 A light meter (LI-COR Biosciences, Germany).

Liquid samples of 100 mL were collected twice a week from the SWW, PBR, settled biomass and effluent for solids and dissolved nutrient quantification. Following ATU addition, the sampling frequency was changed to one sample per day. The samples were filtered (0.45 μm) for dissolved nutrients analysis. TOC, IC and TN concentrations were determined using a Shimadzu TOC-VCSH analyser (Japan) equipped with a TNM-1 chemiluminescence module. Since samples were filtered, the reported TN values correspond to total dissolved nitrogen, encompassing both inorganic nitrogen and dissolved organic nitrogen (DON). N-NH_4^+ was quantified spectrophotometrically at 425 nm using the Nessler method (Shimadzu UV-2550, Japan). N–NO_2^-, N–NO_3^-, and P-PO_4^{3-} concentrations were analysed by ion chromatography (HPLC-IC, Waters 432, conductivity detector, USA).

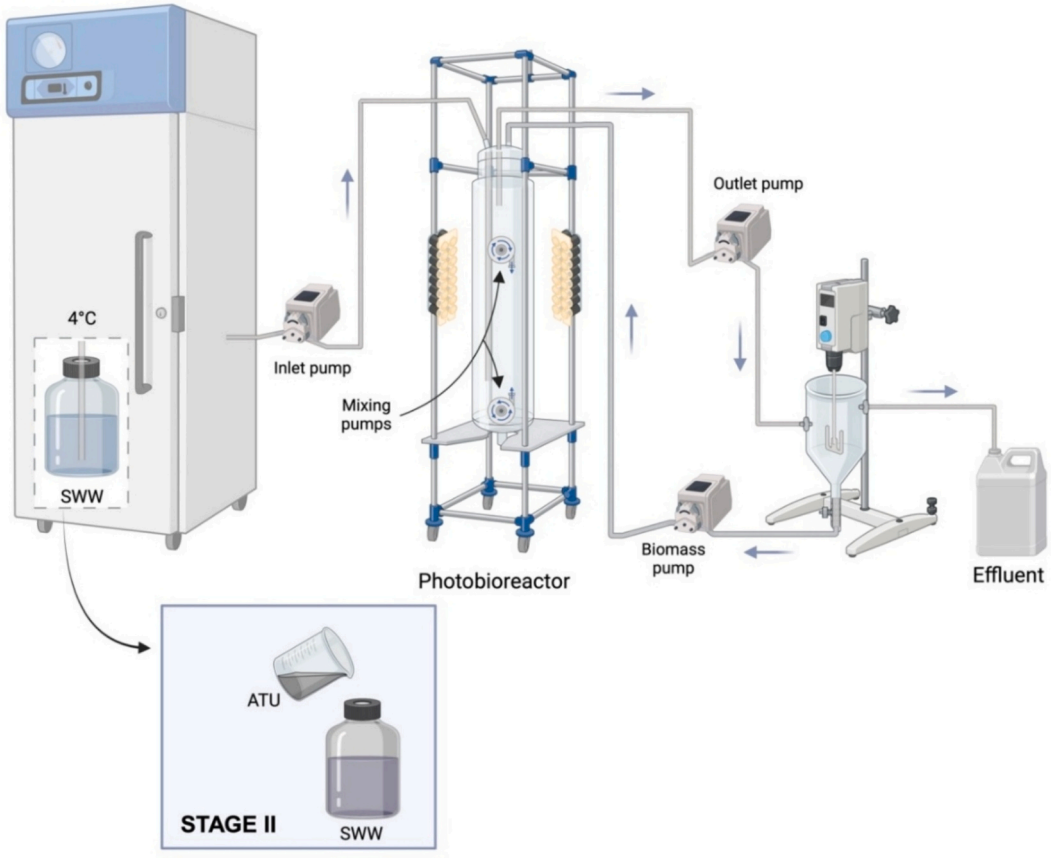

Fig. 1. Schematic diagram of the experimental set-up.

Total suspended solids (TSS) and volatile suspended solids (VSS) concentrations were determined in the PBR, settler and effluent according to standard methods [24].

The concentration of N_2O in the PBR headspace was determined twice a week. A 100 μL gas sample was collected and analysed using a gas chromatograph (Bruker Scion 436, Palo Alto, USA) equipped with an Electron Capture Detector and HS-Q packed column, following the methodology described by [25].

The identification and quantification of the microalgae population were conducted via microscopy examination (OLYMPUS IX70, USA). Samples were fixed with Lugol (5% *v*/v) and formaldehyde solution at (10% v/v), then stored at −20 °C until analysis.

The microbial community analysis was conducted by Novogene company (Novogene, Europe). Genomic DNA was extracted, and the V3-V4 hypervariable region of the 16S rRNA gene was amplified and sequenced on an Illumina platform. Raw sequences were processed using DADA2 for qualify filtering, denoising and amplicon sequence variant (ASV) generation. Taxonomic classification was performed against the SILVA 138 database.

The physiological status of the photosynthetic microorganisms was assessed by measuring the quantum yield (Q_Y) using an AquaPen AP 110-C PAM fluorometer (Photon Systems Instruments, CZ). Prior to measurement, samples were adapted to a dark environment for 15 min.

Additionally, the elemental composition (C, H, N, S, O) of the freeze-dried biomass was determined using an elemental analyser (EA Flash 2000, Thermo Fisher Scientific).

2.5. Calculations

The volumetric biomass productivity was calculated by Eq. 1:

$$BP = \frac{(Q_{withdrawal} \times [VSS]) + (Q_{out} \times [VSS_{out}])}{V_{PBR}} \quad (1)$$

where $Q_{withdrawal}$ is the flowrate (L d^{-1}) withdrawn from settler; Q_{out} is the effluent flowrate (L d^{-1}); $[VSS]$ is the biomass concentration (g L^{-1}) at the bottom of the setter; $[VSS_{out}]$ is the biomass concentration in the effluent and V_{PBR} is the volume of the PBR (m^3).

The concentration of free ammonia [NH_3] (mg N L^{-1}) was estimated from the Anthonisen equation as represented in Eq. 2 [19]:

$$[NH_3] = \frac{[NH_4^+]}{1 + 10^{-pH+0.09018+\frac{2729.92}{T+273}}} \quad (2)$$

where $[NH_4^+]$ is the concentration of ammonium in the PBR; pH is the pH value of the PBR and T is the temperature (°C).

The nitrogen mass balance was calculated according to Eq. 3:

$$Q_{in} \times [TN_{in}] = \left(V_{PBR} \times BP \times \frac{\%N}{100}\right) + (Q_{out} \times [TN_{out}]) + (N_{loss}) \quad (3)$$

where Q_{in} is the flowrate of the inlet SWW (L d^{-1}); $[TN_{in}]$ is the total nitrogen concentration in the inlet SWW (g L^{-1}); V_{PBR} is the PBR volume (m^3); BP is the biomass productivity (g m^{-3} d^{-1}); $\%N$ is the nitrogen content in the biomass (%); Q_{out} is the flowrate of the effluent (L d^{-1}); $[TN_{out}]$ is the total nitrogen concentration in the effluent (g L^{-1}) and N_{loss} represents the unaccounted nitrogen in the mass balance, calculated as the closing term. The N_{loss} was calculated as the difference between the TN input and the sum of TN in the effluent and the N recovered in the biomass.

The carbon mass balance was calculated according to Eq. 4:

$$Q_{in} \times ([TOC_{in}] + [IC_{in}]) = \left(V_{PBR} \times BP \bullet \frac{\%C}{100}\right) + Q_{out} \cdot ([TOC_{out}] + [IC_{out}]) + C_{Loss} \quad (4)$$

where $[TOC_{in}]$ is the total organic carbon concentration in the inlet SWW (L d^{-1}); $[IC_{in}]$ is the inorganic carbon concentration in the inlet SWW (g L^{-1}); $\%C$ is the carbon content in the biomass; $[TOC_{out}]$ is the total organic carbon concentration in the effluent (g L^{-1}); $[IC_{out}]$ is the inorganic carbon concentration in the effluent (g L^{-1}) and C_{Loss} represents the unaccounted carbon in the mass balance.

2.6. Data analysis and visualization

Results are expressed as mean ± standard deviation of the monitored parameters under steady-state operation. After assessing normality with the Shapiro-Wilk test, comparison was made using Student's *t*-test (parametric data) or Brunner-Munzel and Mann-Whitney tests (non-parametric data). All analyses were performed in the Jamovi software (version 2.3.28). BioRender.com was used for creating the Graphical Abstract and Fig. 1.

3. Results and discussion

3.1. Microbial community dynamics

The selective inhibition of AOB with ATU triggered a profound ecological restructuring of the photobioreactor consortium, which reshaped both eukaryotic and prokaryotic communities. This shift in microbial structure was characterized by the suppression of nitrifying and heterotrophic bacteria, which consequently favoured photosynthetic organisms adapted to exploit the newly available ammonium.

A succession on phototrophic microorganisms was observed throughout the operational stages. Initially dominated by *Scenedesmus* sp. (77%), the predominant photosynthetic microorganisms shifted to *Pseudanabaena* sp. (89%) at the end of the Stage I (Fig. 2a). This shift can be attributed to the reduction in HRT to 1 day, which imposed a washout pressure that likely favoured the filamentous morphology of *Pseudanabaena*. The subsequent addition of ATU leaded to NH_4^+ accumulation,

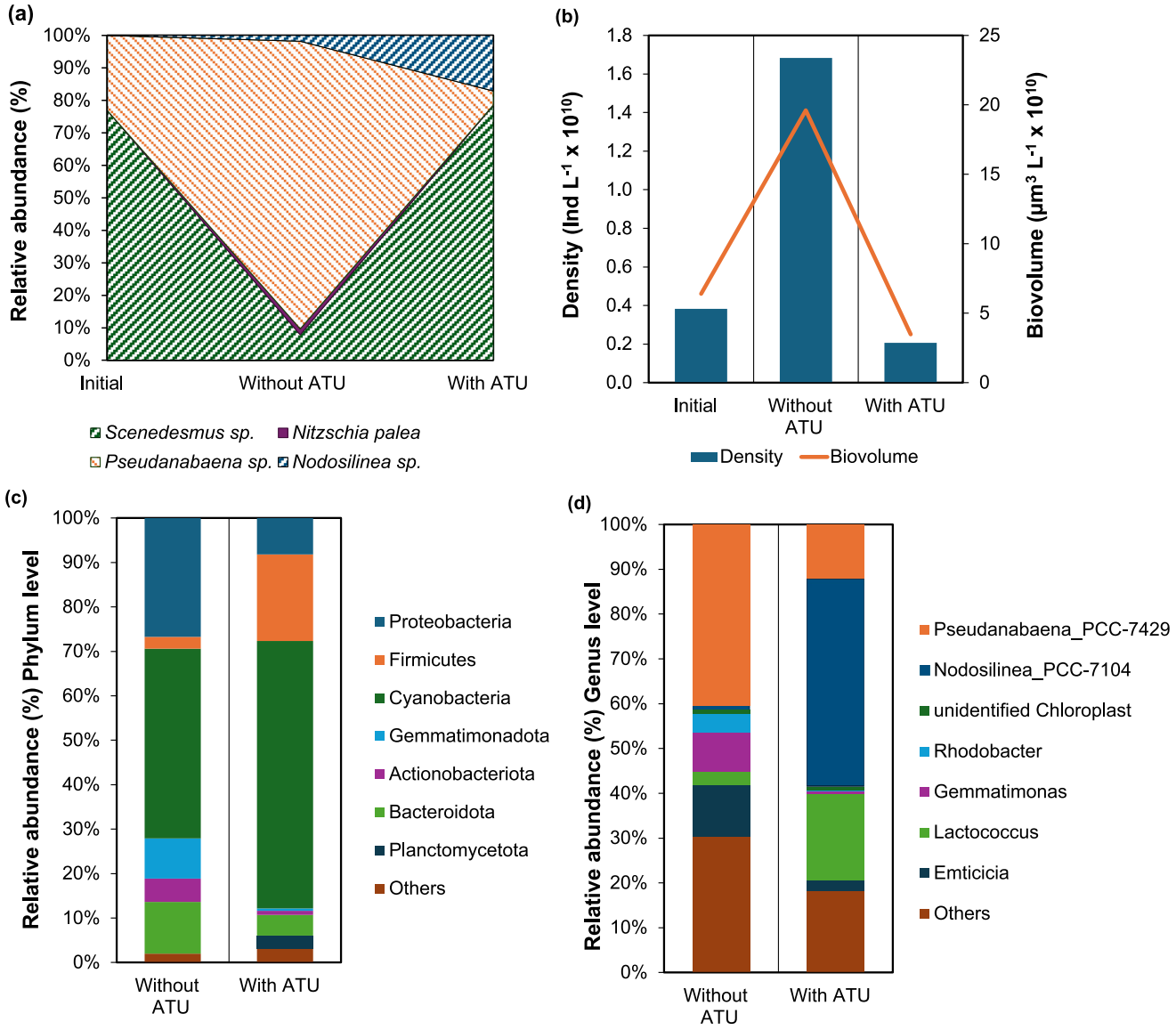

Fig. 2. Microbial community dynamics in the photobioreactor (PBR) across operational stages. Time course of a) the relative abundances (%) of the main microalga species; b) total microalgae densities (blue bars) and total microalgae biovolume (orange line); c) the relative abundance per phyla of bacteria and d) the relative abundance per genus of bacteria. (For interpretation of the references to colour in this figure legend, the reader is referred to the web version of this article.)

favoured *Scenedesmus* sp. and *Nodosilinea* sp. to re-establish as the dominant genera (collectively 96% relative abundance), which became the primary driver of NH_4^+ assimilation. The suppression of *Pseudanabaena* (99% reduction) aligns with ecological principles of nutrient competition and demonstrates its competitive inferiority against specialized ammonium assimilators under the experimental conditions. The competitive advantage of *Scenedesmus* under these conditions aligns with previous report [17] and could be explained by its metabolic flexibility for both photoautotrophic and mixotrophic growth, while *Nodosilinea* benefited from its exclusive dependence on NH_4^+ due to the lack of nitrate reductase [26]. Together, these patterns illustrate how a single operational perturbation can restructure microbial community composition by altering a key environmental filter (NH_4^+ availability), driving succession towards populations with complementary metabolic strategies for ammonium assimilation.

This taxonomic reorganization was further supported by examining cell density and biovolume changes (Fig. 2b). The pronounced decrease in total biovolume following ATU addition was primarily driven by the collapse of *Pseudanabaena* sp., which experienced a 97% reduction in biovolume (from 1.1×10^{11} to 4.2×10^{9} $\mu m^3\ L^{-1}$) and a 99% reduction in cell density. In contrast, *Scenedesmus* sp. maintained stable population density and biovolume, while *Nodosilinea* sp. showed only modest growth.

Experimental evidences confirms that ATU selectively inhibits nitrifying bacteria while preserving microalgal functionality. Rossi et al. [27] demonstrated that microalgal photosynthetic activity was maintained after ATU supplementation in respirometric assays. Similarly, Krustok et al. [17] reported sustained algal growth and even higher chlorophyll *a* concentration in reactors with ATU. Consistent with these findings, a stable photosynthetic performance was observed throughout this ecological shift as shown by Q_Y values consistently exceeding 0.65 in both operational stages. Indeed, the marginal Q_Y reduction from 0.69 ± 0.01 to 0.66 ± 0.02 following ATU addition suggests a minimal impact on photochemical efficiency, further confirming the well-established tolerance of microalgae to ATU [27,28] (Fig. S1a).

The prokaryotic community revealed a parallel restructuring at the phylum level (Fig. 2c). The ATU addition shifted the composition from Cyanobacteria (43%), Proteobacteria (27%) and Bacteroidota (12%) to one dominated by Cyanobacteria (60%), Firmicutes (19%) and a reduced proportion of Proteobacteria (8%). This was characterized by the expansion of *Nodosilinea* (from 1% to 46% of cyanobacteria), likely favoured by the altered nutrient regime, considering its growth is positively influenced by NH_4^+ and its ability of grow in low phosphate concentration [29], outcompeting *Pseudanabaena* (41% to 12% of cyanobacteria, Fig. 2d).

Interestingly, some members of both Proteobacteria and Bacteroidota have been identified as heterotrophic nitrifying bacteria [30,31], which have the ability to produce hydroxylamine, nitrite and nitrate by nitrification using organic carbon for their growth. Declines in the abundance of Bacteriodota (12% to 5%), which important in carbon and nitrogen cycling during wastewater treatment [6], Gemmatimonadota (9% to 1%) and Actinobacteriota (5% to 1%), further underscore the widespread impact of ATU on heterotrophic bacteria involved in nitrogen and carbon transformation. In contrast, Planctomycetota emerged, reaching a 3% relative abundance.

Phylogenetic restructuring was further elucidated by examining abundance shifts at the family level (Fig. S2). The heatmap highlights the specific taxonomic drivers of phylum-level changes. Most notably, the rise of the cyanobacterial family *Nodosilineaceae* indicates its role as the dominant taxon after nitrification inhibition. Conversely, the decline in the abundance of families within the Proteobacteria phylum, such as *Rhodobacteraceae* and *Rhizobiaceae*, visually confirmed the functional reduction of this group, which includes known nitrifying and metabolically versatile heterotrophs crucial for processes like organic carbon degradation [32].

This community turnover was quantified by Amplicon Sequence Variants (ASVs) analysis (Fig. S3), which revealed low overlap (38 shared ASVs). The high proportion of unique ASVs to each condition, 81.4% before versus 84.9% after ATU addition indicates a high degree of dissimilarity and a substantial shift in the microbial community structure induced by nitrification inhibition. Alpha diversity indices (Table S1) confirmed the distinct compositional contrast, showing that the community exhibited a higher overall diversity before ATU addition, as indicated by greater Shannon and Simpson indices. This suggests a well-balanced distribution of taxa abundance. After ATU addition, reduced diversity indices were recorded likely due to the selective environment, while exhibiting a higher taxonomic richness.

Finally, it must be stressed that the prevailing PBR operational conditions may have already been selected for a light-tolerant community. Thus, high light intensities can inhibit some nitrifying bacteria [33]. Therefore, the baseline community prior to ATU addition likely represented a consortium already adapted to photic conditions, with ATU application exerting a strong selective pressure that reshaped community dynamics. The emergence of *Scenedesmus* sp. and *Nodosilinea* sp. highlights the dominance of photosynthetic microorganisms capable nitrogen removal via assimilatory mechanisms.

3.2. Effect of ATU addition on nitrogen removal

The selective inhibition of nitrifying bacteria with ATU was used to infer the contributions of microalgal assimilation and bacterial nitrification and potential denitrification to nitrogen removal. This approach revealed a system where assimilation was the predominant pathway, a trait that was reinforced following the inhibition of competing bacterial processes.

The introduction of ATU into the SWW increased TN concentration from 72.5 ± 6.2 to 87.6 ± 3.7 mg L^{-1}, potentially providing an additional nitrogen source. In this context, the TN removal efficiency in the PBR decreased from 96.7 ± 1.4% to 83.7 ± 1.8% following nitrification inhibition (Fig. 3a). Despite this reduction in nitrogen removal, the post-inhibition removal efficiency aligns with the performance of algal-bacterial PBRs primarily relying on nitrogen assimilation (e.g., 68–79% [7]; 80 ± 6% in enclosed tubular and 92 ± 5% to open PBRs [34]). The relative contribution of assimilation versus nitrification in algal-bacterial systems is highly variable and influenced by operational parameters and community structure [1]. It is important to highlight that while assimilation enables nutrient recovery, its dependence on biomass harvesting and stoichiometric limits constrains the ultimate removal capacity, a role partially played by the nitrification pathway in uninhibited systems. The successful suppression of nitrification was confirmed by the accumulation of NH_4^+ in the PBR, which increased from 0.5 ± 0.1 to 8.9 ± 0.8 mg L^{-1} concomitantly with a reduction in ammonium removal rate from 44.6 to 36.3 mg L^{-1} d^{-1} (Fig. 3b).

The transient accumulation of NO_2^-, which emerged the fourth HRT cycle following ATU addition (Fig. 3c) is an indicator of inhibited NOB activity. Thus, the NO_2^- concentration in the SWW from day 27 until the end of Stage II was 0.65 ± 0.37 mg L^{-1}, and averaged 0.48 ± 0.30 mg L^{-1} in the PBR, which is consistent with minimal NOB activity during this stage. While NO_2^- accumulation can theoretically arise from other pathways (e.g., partial denitrification), this alternative is unlikely in our system given the consistently high dissolved oxygen levels (10.1 ± 1.0 mg O_2 L^{-1}). Therefore, the observed NO_2^- accumulation likely resulted from a combination of low SRT (3 days), inhibitory NH_3 levels and the action of ATU [19].

The calculated free ammonia (NH_3) concentration increased from 0.01 ± 0.01 to 0.22 ± 0.09 mg N L^{-1} as a result of ATU addition. While this concentration remained below the reported inhibitory threshold for microalgae such as *Neochloris oleoabundans* and *Dunaliella tertiolecta* (2.3 and 3.3 mg NH_3 L^{-1}, respectively [35]), it approached levels documented to be toxic for NOB, which can be inhibited at concentrations ranging from 0.1 to 3 mg N L^{-1} [13]. The transient NO_2^- accumulation observed shortly after ATU addition serves as indirect evidence of

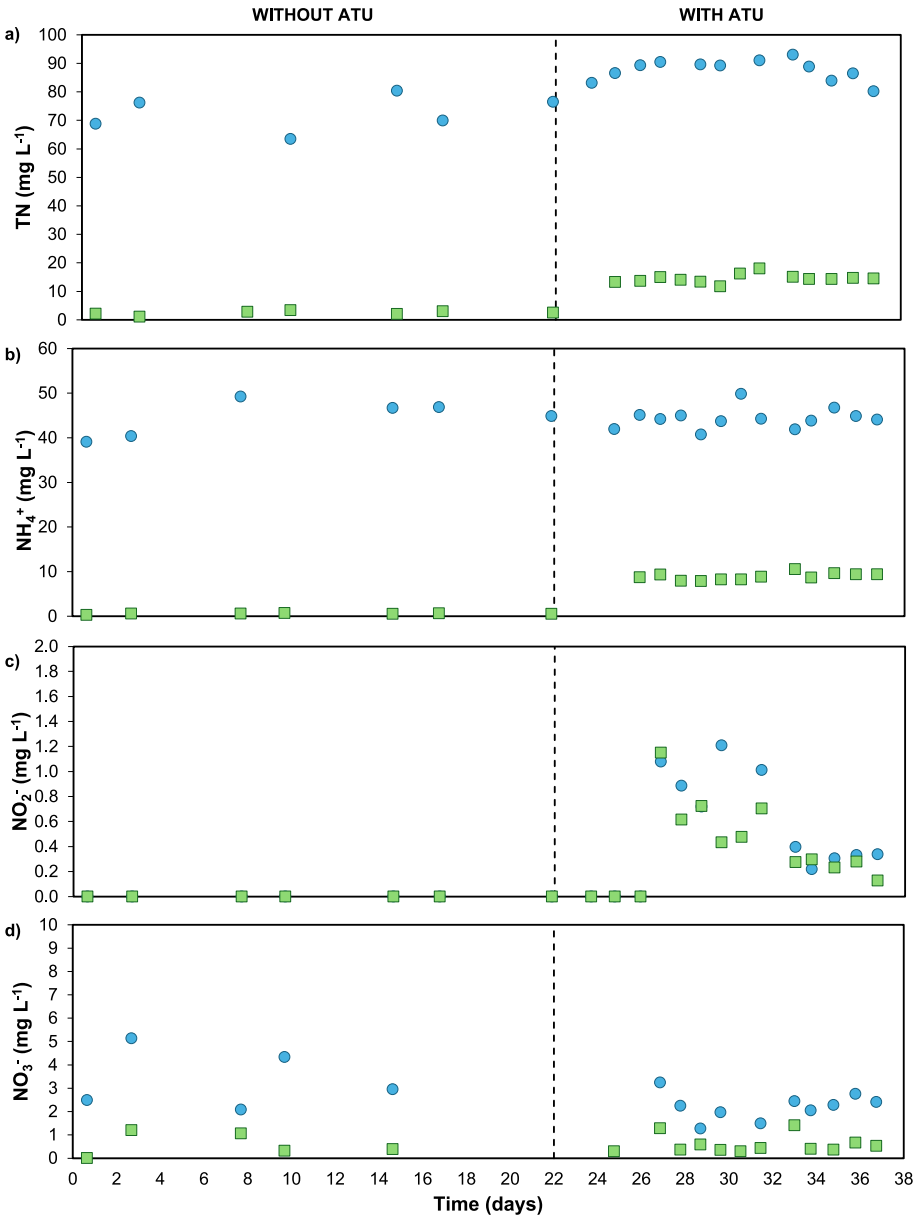

Fig. 3. Nitrogen species concentration. Time course of a) Total nitrogen (TN); b) Ammonium (N-NH_4^+); c) Nitrite (N-NO_2^-); and d) Nitrate (N-NO_3^-) in the PBR (green squares) and in SWW (blue circles). Vertical dashed lines mark stage transitions. (For interpretation of the references to colour in this figure legend, the reader is referred to the web version of this article.)

nitrifying activity prior to ATU addition.

On the other hand, the nitrogen mass balance (Fig. S4) revealed that microalgal assimilation was already the dominant removal mechanism before ATU addition, representing a contribution of 59%. Following inhibition, the newly established consortium (dominated by *Scenedesmus*) increased the relative contribution of nitrogen assimilation to 67%. This result underscore the significant role of the nitrifying community in the uninhibited system, while simultaneously confirming microalgal-bacterial assimilation as the primary removal route under these conditions. This preference is mechanistically explained by microalgae preferentially assimilating NH_4^+ over NO_3^- for biomass synthesis [17], a process facilitated by the absence of the energy-intensive nitrate reduction step required when nitrate is the nitrogen source [18,35].

The functional shift recorded is associated with the observed restructuring of the prokaryotic community. The addition of ATU led to a reduction in the relative abundance of key bacterial phyla, including Proteobacteria and Bacteroidota (Fig. 2c), that represent functionally versatile heterotrophic populations responsible of carbon and nitrogen cycling [30,31]. Bacteroidota are considered primary degraders of polysaccharides [31], while Proteobacteria, primarily made up of gram-negative heterotrophic bacteria [36] capable of utilizing NH_4^+-N and NO_2-N in their metabolism, can have an important role during denitrification [37]. Many organisms within these groups are capable of conducting heterotrophic nitrification and removing nitrogen via aerobic denitrification, generally less efficient than conventional anaerobic denitrification [38].

The pronounced reduction of Proteobacteria and Bacteroidota activity following ATU addition was reflected in the reduced N_{loss} observed in the system, from 0.64 to 0.55 g d^{-1}, as the competing ammonia oxidation pathway was suppressed. However, the remaining N_{loss} of 33% (estimated based on the TN removed) after inhibition suggests the involvement of alternative pathways. This could be attributed to the combined effect of the aforementioned abiotic and heterotrophic

processes, and the activity of resilient or emerging microbial groups. Notably this persistence is potentially linked to the increased abundance of the cyanobacterium *Nodosilinea*, which may perform aerobic nitrification and nitrate reduction [39] or facilitate other nitrogen loss processes. Thus, the post-inhibition N_{loss} likely represents a combination of multiple concurrent biological and physical processes, facilitated by a restructured microbial community.

Importantly, the reduction in TN removal following ATU addition cannot be attributed solely to substrate limitation, as nitrate was consistently present in the influent and nitrite accumulated transiently. Instead, it likely resulted from a combination of factors: the direct loss of nitrification as a removal pathway, the indirect suppression of heterotrophic bacterial groups associated with denitrification and organic carbon turnover, and the incomplete compensation by enhanced algal assimilation.

This finding contrasts with studies by Krustok et al. [17] and Karya et al. [11], where nitrification was identified as the dominant route for NH_4^+ removal. The discrepancy can be attributed to key operational differences, most notably the significantly higher light intensity (316.6 μmol m^{-2} s^{-1}) and continuous photoperiod (24 h) in our work, compared to 100 μmol m^{-2} s^{-1} under a 16:8 h light:dark cycle [17] and 63 μmol m^{-2} s^{-1} used by these authors [11]. These conditions strongly favour photosynthetic activity and assimilatory uptake by microalgae over bacterial nitrification. Furthermore, the different operational HRT, SRT and C:N:P ratios among studies likely selected for a microbial community dominated by organisms with high assimilatory capacity, as evidenced by the dominance of *Scenedesmus* sp. This view is supported by Bankston et al. [40], who found algal assimilation to be nearly twice as higher as nitrification on treatment of poultry litter slurry anaerobic digestate. These data confirm that the nitrification process can directly compete with and limit microalgae growth, a phenomenon previously suggested in lab-scale and pilot-scale studies [41]. The demonstrated dominance of nitrogen assimilation shows that microbial community function, and consequently nutrient removal pathways, can be strategically controlled by tailoring the operational environment to enhance nitrogen recovery efficiency.

In this study, N_2O emissions remained negligible (77.0 ± 19.7 ppm_v in the PBR headspace; equivalent to 1.1 mg N L^{-1}), representing less than 0.1% of total nitrogen losses. This low production correlates with the operational conditions featuring high DO levels, negligible NO_2^- accumulation and the suppression of the nitrification pathway (during Stage II). These findings align with Kim et al. [42], who demonstrated

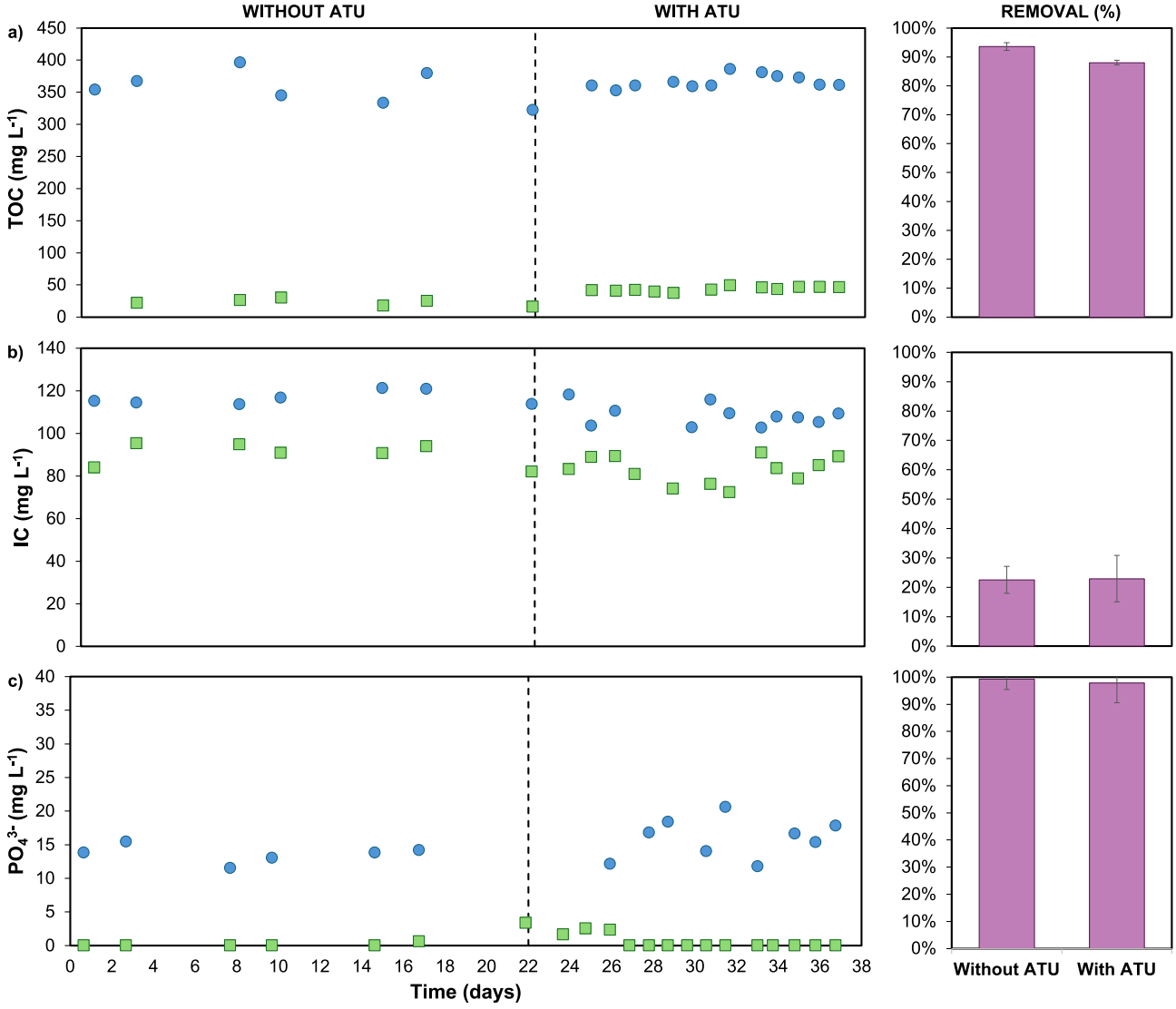

Fig. 4. Carbon, phosphate, and removal efficiency. Time course of the (a) TOC, (b) IC, and (c) $P\text{-}PO_4^{3-}$ concentrations in the PBR (green squares) and SWW (blue circles). The corresponding removal efficiency (%) for each parameter is shown as magenta columns. (For interpretation of the references to colour in this figure legend, the reader is referred to the web version of this article.)

that N_2O emission during nitrification largely depend on AOB activity. The complete mechanisms of N_2O formation remain debated, however, it is established that production occurs through both autotrophic nitrification (via AOB activity) and incomplete heterotrophic denitrification, with enhanced emissions under conditions of low DO, elevated NO_2^- concentrations, and low C/N ratios [43].

3.3. Effect of ATU addition on carbon and phosphorus removal

The addition of ATU induced a shift in carbon cycling in the algal-bacterial PBR dynamics. The decrease in TOC removal efficiency from 94 ± 1 to 88 ± 1% (Fig. 4a) suggests a partial suppression of heterotrophic activity responsible for organic carbon mineralization. Furthermore, the observed decrease in TOC removal efficiency suggests a secondary effect of suppression of heterotrophic activity, while the maintained overall biomass productivity and quantum yield (Q_Y) confirm that the core photosynthetic function was preserved, as supported by previous literature [17]. This may be a secondary consequence of nitrification inhibition. While primary action of ATU is inhibiting the ammonia monooxygenase (AMO), a potential broader effect can also chelate the copper cofactor in multiple microbial enzymes, potentially inhibiting the metabolic activity of heterotrophs [44]. The observed reduction in the relative abundance of key heterotrophic phyla, specifically Firmicutes and Bacteroidota, which typically remove TN by consuming TOC under anoxic conditions [37], likely impaired organic carbon mineralization, leaving a fraction of TOC bioavailable in the PBR.

This primary disruption of nitrogen transformations and heterotrophic metabolism cascaded into a reconfiguration of carbon processing. The carbon mass balance (Fig. S4) revealed an important metabolic shift. The efficiency of carbon assimilation into biomass increased from 65% to 80% following ATU addition. This suggests that the inhibition of heterotrophic bacteria may have reduced competition for organic carbon, thereby increasing its availability for other metabolisms, such as the mixotrophic microalga *Scenedesmus*. The sustained TOC removal during the period of *Scenedesmus* dominance is consistent with its effectively assimilating both the increased NH_4^+ and available organic carbon. This correlation suggests a possible role for *Scenedesmus* in organic carbon uptake under these conditions. Given the potential of heterotrophic bacteria from the Rhodobacteraceae family consuming organic carbon, the observed decline in the group, along with Proteobacteria, and the rise of Firmicutes, provides a taxonomic explanation for the observed restructuration of carbon metabolism pathways in the consortium. Furthermore, the alteration of nitrogen availability following ATU inhibition induced a shift in the microbial community structure, favouring the dominance of versatile microalgae like *Scenedesmus* sp., while the bloom of cyanobacteria highlights the functional redundancy for nutrient assimilation within the consortium.

The carbon mass balance further supports this mechanism. While the total carbon concentration in the effluent remained virtually constant (113.3 ± 10.1 mg L^{-1}; $p > 0.05$), the C_{Loss} decreased from 35% to 20%, indicating a suppression of heterotrophic activity and the redirection of carbon to algal assimilation. The increase in the organic carbon required per unit of ammonium removed, from 7.6 to 9.0 mg_{TOC} $mg^{-1}_{N\text{-}NH4+}$, reflects this transition from a community predominantly dominated by heterotrophic bacteria to one dominated by mixotrophic algae with a different carbon-to-nitrogen utilization ratio. Furthermore, the consistent IC removal efficiency, averaged 23 ± 7% along both operational stages (Fig. 4b), reinforces that photosynthetic assimilation by microalgae was the primary mechanism for IC removal.

Finally, it must be stressed that even under the selective suppression of bacterial activity and the 1-day HRT, the system maintained a high TOC removal efficiency >89%. In this context, Posadas et al. [34] reported a similar range of TOC removals (63–97%) in an enclosed tubular PBR and in an open biofilm PBR operating at longer HRTs (5–10 days), underscoring the robustness of the carbon removal pathway in the algal-bacterial column photobioreactor herein tested.

On the other hand, the PBR supported consistently high P-PO_4^{3-} removal efficiencies of 98 ± 4% without ATU and of 97 ± 7% with ATU (Fig. 4c), with no statistically significant difference between stages ($p > 0.05$).This indicates that nitrification activity exerted a negligible impact on phosphate removal, consistent with the findings of Krustok et al. [17] at low P concentrations. Despite microalgae are able to assimilate N under P-limited conditions [17], nitrifying bacteria growth can be significantly affected [13]. Notably, the N:P ratios (5:1 without ATU and 6:1 with ATU) are in agreement with the optimal 5:1–8:1 range needed to sustain high removal efficiencies by *Scenedesmus* sp. [45], suggesting that the nutrient balance was theoretically favourable for a concurrent N and P removal. Furthermore, given that the pH remained below 8 (Fig. 5a), a range where significant phosphate precipitation, it can be inferred that the high phosphorus removal efficiency was primarily driven by assimilation into biomass.

3.4. Effect of ATU addition on photobioreactor performance and biomass productivity

The PBR maintained stable bioremediation performance throughout the experimental period, demonstrating system resilience to the imposed metabolic inhibition (Fig. 5). The pH remained constant at 7.4 ± 0.2 without external control and was unaffected by ATU-based nitrification inhibition. Similarly, the DO concentration remained stable at 10.4 ± 2.1 mg L^{-1} across both operational stages. The high stability of DO following ATU addition can be attributed to the high turbulence in the algal cultivation broth mediated by the two submerged pumps, which allow stripping out the excess of DO not consumed by nitrifiers in Stage II.

Temperature averaged 30.3 ± 1.7 °C, which could potentially favour AOB growth over microalgae [19]. However, as both experimental stages experienced the same averaged temperature, the comparative assessment of nitrification inhibition remains valid. The constant light irradiance may have provided partial compensation by inhibiting nitrifying bacteria [19], though this effect was consistent across both stages.

The operational strategy of maintaining the biomass concentration below 2 gTSS L^{-1} in the PBR was successful, as reflected in the stable VSS profiles, where median values remained similar between operational stages (Fig. S1b). This strategy is known to favour bacterial communities that exhibit faster growth rates compared to microalgae [46]. Despite the significant ecological shift, the selective inhibition of nitrifiers by ATU did not lead to a statistically significant effect on the overall biomass productivity ($p > 0.05$), which increased from 563 ± 118 to 672 ± 163 g m^{-3} d^{-1} (Fig. S1c). This stability in productivity was accompanied by a consistent elemental composition of the biomass, with nitrogen and carbon contents remaining at 7.5 ± 0.1% and 42.7 ± 0.7% in Stage II compared to 7.6 ± 0.1% and 43.8 ± 0.5% in Stage I, respectively.

The alteration of metabolic dynamics by ATU points towards an inhibition beyond nitrifiers. This is evidenced by a decrease in the specific ammonium removal rate from 79.1 to 52.9 mg NH_4^+ g^{-1} $_{biomass}$, indicating that a less efficient metabolism occurred simultaneously with an overall decreased in total TOC removal. This finding suggests that the resulting community is not only less efficient in its nitrogen metabolism but also less effective at consuming the available organic carbon substrate, reinforcing the hypothesis of an inhibitory effect of ATU on heterotrophic biomass.

4. Conclusion

This study demonstrates that nitrogen removal in a single-stage algal-bacteria PBR was governed by concurrent action of assimilation and nitrification. The reduction in total nitrogen removal upon nitrification inhibition suggests that this pathway likely weakened a

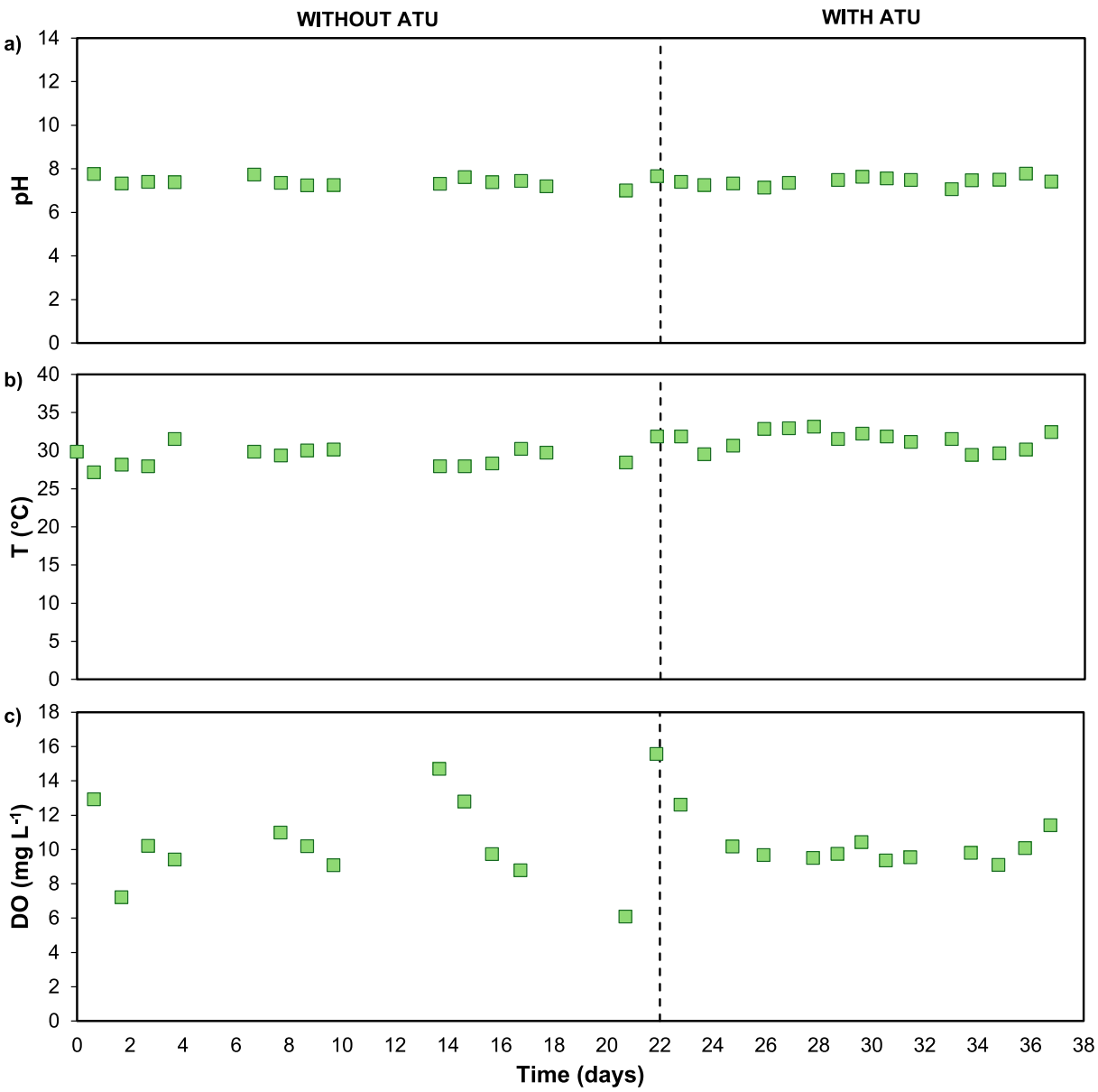

Fig. 5. Physicochemical parameters in the PBR. Time course of the (a) pH, (b) temperature and (c) dissolved oxygen concentration in the algal-bacterial broth during PBR operation.

subsequent denitrification process. The strategic nitrification inhibition with ATU was pivotal in decoupling these processes, confirming microalgal assimilation as the dominant mechanism under the tested condition and revealing the critical role of bacterial community structure. The maintenance of nitrogen removal performance after ATU addition indicated that other microorganisms beyond strict nitrifiers contributed to nitrogen removal, suggesting a degree of functional redundancy within the consortium, where heterotrophic bacteria and other autotrophs likely played a complementary role. Furthermore, the increase in NH_4^+ availability following inhibition induced a shift in the microbial community structure, favouring versatile microalgae like *Scenedesmus* sp., while the bloom of cyanobacteria highlights the functional redundancy for nutrient assimilation within the consortium.

A key advantage of the dominant nitrogen assimilatory mechanisms is the efficient direction of nitrogen into biomass, yielding a product with high nutrient content better suited for valorisation purposes. Furthermore, this process entailed consistently low N_2O emissions regardless of the operational stage, underscoring its secondary environmental benefit. Ultimately, the findings confirm that the balance between nitrogen assimilation and oxidation is adjustable, highlighting the flexibility of microalgae-bacteria consortia for advancing circular wastewater treatment models focused on nutrient recovery. While ATU supplementation was used as a proof-of-concept tool, practical application would rely on sustainable operational controls to reduce nitrification and favour the process towards nutrient recovery. To further refine this strategy and completely uncover the mechanisms, future research should employ advanced tools such as isotopic tracers to partition nutrient fluxes. Complementary techniques, including photosynthetic pigment analysis or 18S rRNA gene quantification should be used to precisely elucidate the contributions of algal and bacterial groups, and to quantify algal-specific growth rates, thereby enabling modelling and optimization.

CRediT authorship contribution statement

Thalita Lacerda dos Santos: Writing – original draft, Investigation, Conceptualization. **Laura Vargas-Estrada:** Writing – review & editing, Validation, Supervision, Conceptualization. **Saúl Blanco:** Investigation,

Formal analysis. **Gustavo Henrique Ribeiro da Silva:** Writing – review & editing, Project administration, Funding acquisition. **Raúl Muñoz:** Writing – review & editing, Validation, Supervision, Resources, Project administration, Funding acquisition, Conceptualization.

Declaration of competing interest

The authors declare that they have no known competing financial interests or personal relationships that could have appeared to influence the work reported in this paper.

Acknowledgements

The scholarship granted by the Brazilian Federal Agency for Support and Evaluation of Graduate Education (CAPES), within the scope of CAPES-PrInt Program (Project number 88887.194785/2018–00; Process number 88887.892272/2023–00) is gratefully acknowledged. Laura Vargas-Estrada acknowledges the Marie Skłodowska-Curie Individual Fellowship (Grant Agreement No 101148763). The National Council for Scientific and Technological Development (CNPq; Process number 308663/2021–7) is gratefully acknowledged.

Appendix A. Supplementary data

Supplementary data to this article can be found online at https://doi.org/10.1016/j.jwpe.2026.109975.

Data availability

No data was used for the research described in the article.

References

[1] A. Fallahi, F. Rezvani, H. Asgharnejad, E. Khorshidi Nazloo, N. Hajinajaf, B. Higgins, Interactions of microalgae-bacteria consortia for nutrient removal from wastewater: a review, Chemosphere 272 (2021) 129878, https://doi.org/10.1016/j.chemosphere.2021.129878.

[2] S. Rahimi, O. Modin, I. Mijakovic, Technologies for biological removal and recovery of nitrogen from wastewater, Biotechnol. Adv. 43 (2020) 107570, https://doi.org/10.1016/j.biotechadv.2020.107570.

[3] Y. Yan, H. Lu, J. Zhang, S. Zhu, Y. Wang, Y. Lei, R. Zhang, L. Song, Simultaneous heterotrophic nitrification and aerobic denitrification (SND) for nitrogen removal: a review and future perspectives, Environ. Adv. 9 (2022) 100254, https://doi.org/10.1016/j.envadv.2022.100254.

[4] S.F. Mohsenpour, S. Hennige, N. Willoughby, A. Adeloye, T. Gutierrez, Integrating micro-algae into wastewater treatment: a review, Sci. Total Environ. 752 (2021) 142168, https://doi.org/10.1016/j.scitotenv.2020.142168.

[5] L. Tang, Y. Zhang, M. Gao, X. Wang, Simultaneous Nitrification–Endogenous Denitrification with Phosphorus Removal Sustained by Aeration-Free Filamentous Microalgal–Bacterial Granular Sludge for Low C/N Wastewater Treatment, ACS EST Eng. (2025), https://doi.org/10.1021/acsestengg.4c00833.

[6] Q. Liu, X. Lei, J. Li, L. Chu, F. Wang, H. Shan, F. Hu, Microbial communities and nitrogen cycling in *Litopenaeus vannamei* and *Mercenaria mercenaria* polyculture ponds, Aquacult. Rep. 33 (2023) 101769, https://doi.org/10.1016/j.aqrep.2023.101769.

[7] C. Alcántara, J.M. Domínguez, D. García, S. Blanco, R. Pérez, P.A. García-Encina, R. Muñoz, Evaluation of wastewater treatment in a novel anoxic–aerobic algal–bacterial photobioreactor with biomass recycling through carbon and nitrogen mass balances, Bioresour. Technol. 191 (2015) 173–186, https://doi.org/10.1016/j.biortech.2015.04.125.

[8] L. Peng, Y. Li, Q. Li, C. Liang, M. Nasr, Y. Xu, Y. Liu, Y. Zhou, The effect of free ammonia on ammonium removal and N2O production in a consortium of microalgae and partial nitritation cultures, Chem. Eng. J. 474 (2023) 145572, https://doi.org/10.1016/j.cej.2023.145572.

[9] C. Alcántara, E. Posadas, B. Guieysse, R. Muñoz, Microalgae-based Wastewater Treatment. 439–455 (2015), https://doi.org/10.1016/b978-0-12-800776-1.00029-7.

[10] Shinichi Akizuki, Akizuki, S., Masatoshi Kishi, Kishi, M., Germán Cuevas-Rodríguez, Cuevas-Rodríguez, G., Tatsuki Toda, Toda, T.: corrigendum to "effects of different light conditions on ammonium removal in a consortium of microalgae and partial nitrifying granules" [water res. 171 (2020) 115445], Water Res. 175 (115778) (2020), https://doi.org/10.1016/j.watres.2020.115778.

[11] N.G.A.I. Karya, N.P. van der Steen, P.N.L. Lens, Photo-oxygenation to support nitrification in an algal–bacterial consortium treating artificial wastewater, Bioresour. Technol. 134 (2013) 244–250, https://doi.org/10.1016/j.biortech.2013.02.005.

[12] B. Zhang, W. Li, Y. Guo, Z. Zhang, W. Shi, F. Cui, P.N.L. Lens, J.H. Tay, Microalgal-bacterial consortia: from interspecies interactions to biotechnological applications, Renew. Sust. Energ. Rev. 118 (2020) 109563, https://doi.org/10.1016/j.rser.2019.109563.

[13] J. González-Camejo, S. Aparicio, M. Pachés, L. Borrás, A. Seco, Comprehensive assessment of the microalgae-nitrifying bacteria competition in microalgae-based wastewater treatment systems: relevant factors, evaluation methods and control strategies, Algal Res. 61 (2022) 102563, https://doi.org/10.1016/j.algal.2021.102563.

[14] L. Vargas-Estrada, A. Longoria, P.U. Okoye, P.J. Sebastian, Energy and nutrients recovery from wastewater cultivated microalgae: assessment of the impact of wastewater dilution on biogas yield, Bioresour. Technol. 341 (2021) 125755, https://doi.org/10.1016/j.biortech.2021.125755.

[15] M.E. Wali, S.R. Golroudbary, Andrzej Kraslawski, Andrzej Kraslawski, A. Kraslawski, Circular economy for phosphorus supply chain and its impact on social sustainable development goals, Sci. Total Environ. 777 (2021) 146060, https://doi.org/10.1016/j.scitotenv.2021.146060.

[16] H. Al-Jabri, P. Das, S. Khan, M. Thaher, M. AbdulQuadir, Treatment of wastewaters by microalgae and the potential applications of the produced biomass—a review, Water 13 (2021) 27, https://doi.org/10.3390/w13010027.

[17] I. Krustok, M. Odlare, J. Truu, E. Nehrenheim, Inhibition of nitrification in municipal wastewater-treating photobioreactors: effect on algal growth and nutrient uptake, Bioresour. Technol. 202 (2016) 238–243, https://doi.org/10.1016/j.biortech.2015.12.020.

[18] K. Nishi, S. Akizuki, T. Toda, T. Matsuyama, J. Ida, Advanced light-tolerant microalgae-nitrifying bacteria consortia for stable ammonia removal under strong light irradiation using light-shielding hydrogel, Chemosphere 297 (2022) 134252, https://doi.org/10.1016/j.chemosphere.2022.134252.

[19] J. González-Camejo, P. Montero, S. Aparicio, M.V. Ruano, L. Borrás, A. Seco, R. Barat, Nitrite inhibition of microalgae induced by the competition between microalgae and nitrifying bacteria, Water Res. 172 (2020) 115499, https://doi.org/10.1016/j.watres.2020.115499.

[20] P. Ginestet, J.-M. Audic, V. Urbain, J.-C. Block, Estimation of nitrifying bacterial activities by measuring oxygen uptake in the presence of the metabolic inhibitors allylthiourea and Azide, Appl. Environ. Microbiol. 64 (1998) 2266–2268, https://doi.org/10.1128/AEM.64.6.2266-2268.1998.

[21] L. Ferro, M. Colombo, E. Posadas, C. Funk, R. Muñoz, Elucidating the symbiotic interactions between a locally isolated microalga Chlorella vulgaris and its co-occurring bacterium Rhizobium sp. in synthetic municipal wastewater, J. Appl. Phycol. 31 (2019) 2299–2310, https://doi.org/10.1007/s10811-019-1741-1.

[22] E.G. Hoyos, R. Kuri, T. Toda, R. Muñoz, Innovative design and operational strategies to improve CO2 mass transfer during photosynthetic biogas upgrading, Bioresour. Technol. 391 (2024) 129955, https://doi.org/10.1016/j.biortech.2023.129955.

[23] T.L. dos Santos, L. Vargas-Estrada, S. Blanco, G.H.R. da Silva, R. Muñoz, Influence of operational parameters on the performance of domestic wastewater treatment in a single-stage algal-bacterial column photobioreactor, Algal Res. 92 (2025) 104417, https://doi.org/10.1016/j.algal.2025.104417.

[24] Standard Methods for the Examination of Water and Wastewater, American Public Health Association, 2017, https://doi.org/10.2105/SMWW.2882.

[25] O.D. Frutos, I.A. Arvelo, R. Pérez, G. Quijano, R. Muñoz, Continuous nitrous oxide abatement in a novel denitrifying off-gas bioscrubber, Appl. Microbiol. Biotechnol. 99 (2015) 3695–3706, https://doi.org/10.1007/s00253-014-6329-8.

[26] L. Yi, R. Solanki, M. Strous, In search of the pH limit of growth in halo-alkaliphilic cyanobacteria, Environ. Microbiol. Rep. 16 (2024) e13323, https://doi.org/10.1111/1758-2229.13323.

[27] S. Rossi, M. Bellucci, F. Marazzi, V. Mezzanotte, E. Ficara, Activity assessment of microalgal-bacterial consortia based on respirometric tests, Water Sci. Technol. 78 (2018) 207–215, https://doi.org/10.2166/wst.2018.078.

[28] A. Sánchez-Zurano, C. Gómez-Serrano, F.G. Acién-Fernández, J.M. Fernández-Sevilla, E. Molina-Grima, A novel photo-respirometry method to characterize consortia in microalgae-related wastewater treatment processes, Algal Res. 47 (2020) 101858, https://doi.org/10.1016/j.algal.2020.101858.

[29] S. Yadav, G.B. Anam, Y.-H. Ahn, Influence of abiotic factors on the growth of Cyanobacteria isolated from Nakdong River, south Korea1, J. Phycol. 57 (2021) 874–885, https://doi.org/10.1111/jpy.13143.

[30] K. Wang, D. Yan, X. Chen, Z. Xu, W. Cao, H. Li, New insight to the enriched microorganisms driven by pollutant concentrations and types for industrial and domestic wastewater via distinguishing the municipal wastewater treatment plants, Environ. Pollut. 361 (2024) 124789, https://doi.org/10.1016/j.envpol.2024.124789.

[31] P. Lapébie, V. Lombard, E. Drula, N. Terrapon, B. Henrissat, Bacteroidetes use thousands of enzyme combinations to break down glycans, Nat. Commun. 10 (2019) 2043, https://doi.org/10.1038/s41467-019-10068-5.

[32] A. Morillas-España, A. Sánchez-Zurano, T. Lafarga, M. del Mar Morales-Amaral, C. Gómez-Serrano, F.G. Acién-Fernández, C.V. González-López, Improvement of wastewater treatment capacity using the microalga *Scenedesmus* sp. and membrane bioreactors, Algal Res. 60 (2021) 102516, https://doi.org/10.1016/j.algal.2021.102516.

[33] G. Vargas, A. Donoso-Bravo, C. Vergara, G. Ruiz-Filippi, Assessment of microalgae and nitrifiers activity in a consortium in a continuous operation and the effect of oxygen depletion, Electron. J. Biotechnol. 23 (2016) 63–68, https://doi.org/10.1016/j.ejbt.2016.08.002.

[34] E. Posadas, P.A. García-Encina, A. Domínguez, I. Díaz, E. Becares, S. Blanco, R. Muñoz, Enclosed tubular and open algal–bacterial biofilm photobioreactors for

carbon and nutrient removal from domestic wastewater, Ecol. Eng. 67 (2014) 156–164, https://doi.org/10.1016/j.ecoleng.2014.03.007.
[35] W.S. Chai, C.H. Chew, H.S.H. Munawaroh, V. Ashokkumar, C.K. Cheng, Y.-K. Park, P.L. Show, Microalgae and ammonia: a review on inter-relationship, Fuel 303 (2021) 121303, https://doi.org/10.1016/j.fuel.2021.121303.
[36] K. Wang, D. Yan, X. Chen, Z. Xu, W. Cao, H. Li, New insight to the enriched microorganisms driven by pollutant concentrations and types for industrial and domestic wastewater via distinguishing the municipal wastewater treatment plants, Environ. Pollut. 361 (2024) 124789, https://doi.org/10.1016/j.envpol.2024.124789.
[37] X. Yue, X. Xiao, J. Liang, Y. Lin, K. Xiao, K. Che, Firmicutes and Bacteroidetes as the dominant microorganisms for ammonium nitrogen wastewater treatment with a low C/N ratio in BCOR, J. Water Process Eng. 65 (2024) 105851, https://doi.org/10.1016/j.jwpe.2024.105851.
[38] V. Baskaran, P.K. Patil, M.L. Antony, S. Avunje, V.T. Nagaraju, S.D. Ghate, S. Nathamuni, N. Dineshkumar, S.V. Alavandi, K.K. Vijayan, Microbial community profiling of ammonia and nitrite oxidizing bacterial enrichments from brackishwater ecosystems for mitigating nitrogen species, Sci. Rep. 10 (2020) 5201, https://doi.org/10.1038/s41598-020-62183-9.
[39] K. Phyu, S. Zhi, D.W. Graham, Y. Cao, X. Xu, J. Liu, H. Wang, K. Zhang, Impact of indigenous vs. cultivated microalgae strains on biomass accumulation, microbial community composition, and nutrient removal in algae-based dairy wastewater treatment, Bioresour. Technol. 426 (2025) 132349, https://doi.org/10.1016/j.biortech.2025.132349.
[40] E. Bankston, Q. Wang, B.T. Higgins, Algae support populations of heterotrophic, nitrifying, and phosphate-accumulating bacteria in the treatment of poultry litter anaerobic digestate, Chem. Eng. J. 398 (2020) 125550, https://doi.org/10.1016/j.cej.2020.125550.
[41] J. González-Camejo, S. Aparicio, M.V. Ruano, L. Borrás, R. Barat, J. Ferrer, Effect of ambient temperature variations on an indigenous microalgae-nitrifying bacteria culture dominated by *Chlorella*, Bioresour. Technol. 290 (2019) 121788, https://doi.org/10.1016/j.biortech.2019.121788.
[42] S.-W. Kim, M. Miyahara, S. Fushinobu, T. Wakagi, H. Shoun, Nitrous oxide emission from nitrifying activated sludge dependent on denitrification by ammonia-oxidizing bacteria, Bioresour. Technol. 101 (2010) 3958–3963, https://doi.org/10.1016/j.biortech.2010.01.030.
[43] B.-J. Ni, M. Ruscalleda, C. Pellicer-Nàcher, B.F. Smets, Modeling nitrous oxide production during biological nitrogen removal via nitrification and denitrification: extensions to the general ASM models, Environ. Sci. Technol. 45 (2011) 7768–7776, https://doi.org/10.1021/es201489n.
[44] M. Yi, Q. Sheng, Q. Sui, H. Lu, β-Blockers in the environment: distribution, transformation, and ecotoxicity, Environ. Pollut. 266 (2020) 115269, https://doi.org/10.1016/j.envpol.2020.115269.
[45] L. Xin, H. Hong-ying, G. Ke, S. Ying-xue, Effects of different nitrogen and phosphorus concentrations on the growth, nutrient uptake, and lipid accumulation of a freshwater microalga *Scenedesmus* sp, Bioresour. Technol. 101 (2010) 5494–5500, https://doi.org/10.1016/j.biortech.2010.02.016.
[46] J. González-Camejo, S. Aparicio, A. Jiménez-Benítez, M. Pachés, M.V. Ruano, L. Borrás, R. Barat, A. Seco, Improving membrane photobioreactor performance by reducing light path: operating conditions and key performance indicators, Water Res. 172 (2020) 115518, https://doi.org/10.1016/j.watres.2020.115518.